Chapter 2

Study of metal-coated D-shaped RI SPR optical fiber sensor

In this chapter, I present a detailed study on surface plasmon resonance (SPR)-based D-shaped single-mode optical fiber sensor for the range of refractive index (RI) 1.33–1.42 sensing using the finite element method (FEM). Gold (Au), silver (Ag), and copper (Cu) metal layers have used separately to investigate the performance of proposed sensor employed with SPR conditions. I observe the higher sensitivity for the Au layer in comparison to Ag and Cu layers. Sensor with Au layer with 50 nm thickness shows the average sensitivity of 5855 nm/RIU with maximum sensitivity of 15,200 nm/RIU and resolution 1.780 × 10^{-5} RIU. The sensing performance of the sensor sequentially decreases with Ag and Cu layers. The proposed optical fiber sensors with high sensing performance can be utilized as RI sensors for different chemical and biological sensing.

2.1 Introduction

In the recent decades, surface plasmon resonance (SPR) - based sensors have enticed major attention because of their attractive features in terms of higher sensitivity, very fast response time, label-free detection, and precise optical sensing for various chemical, biological, and physical parameters. Many sensors such as temperature sensors, pH sensors, RI sensors, biosensors, etc. have been designed based on the SPR phenomenon[86 87 88]. SPR phenomenon is a resonant oscillation of the charged particles at the metal–dielectric interface stimulated by incident light. In order to obtain the resonance condition, momentum, and energy of the incident light should match to momentum and energy of the surface plasmon wave, which provides more sensitivity towards a slight variation in the dielectric of analyte. Therefore, a small change in the analyte refractive index (RI) can be detected by the SPR condition. The condition of resonance depends on the properties of an incident wave such as wavelength, incident angle, and also on refractive index (RI) of analyte and metal[89 90 91 92 93]. Kretschmann's configuration[50] based on total internal reflection is the most promising technique to observe the SPR condition so far. In their proposed design, a thin layer of metal was deposited on a prism, having higher dielectric constant, and analyte was in contact with the metal layer. Such types of SPR-based sensors have many demerits such as bulky in size, inability for remote sensing, costly fabrication process, and complex operating. However, SPR optical fiber sensors provide many benefits over the prism sensors in terms of higher sensitivity, simple and flexible in design, cheap fabrication, advanced for remote sensing, real-time detection, and can be useful to environmental, biochemical, and monitoring of industrial area[50 94 95 96]. SPR-based sensing in optical fiber has been studied both theoretically and experimentally for various types of designs such as D-shaped fibers[78], U bent fiber[79], microstructure optical fiber[80 16] and some other research works[97 98 99 100].

In this work, I have investigated the performance of broad range SPR-based D-shaped optical fiber RI sensor. Metals gold (Au), silver (Ag), and copper (Cu) have incorporated separately on the fiber core to get the SPR condition for RI sensing. I have applied the wavelength interrogation method to the study of sensing performance of the considered sensors. The thickness of metal layers is an important factor to observe the sensitivity variations. So, we have demonstrated the resonance wavelength, confinement loss, and sensitivity at different layer thicknesses of the metals. Resonance wavelength, confinement loss, and sensitivity spectra have shown for different refractive indices. I have also studied the figure of merit (FOM) of the proposed sensor. In last, I have summarized the results.

2.2 Theoretical description

I have used the well-known single-mode D-shaped optical fiber structure of the core diameter 8.2 μm and the cladding diameter 125 μm for the simulation of the sensor. Side polishing and laser micro-machine techniques are most suitable for the fabrication of D-shaped fiber and control the depth of fiber[101]. A metal layer is covered with the sensing material, and its cross-section and side view are shown in Fig. 2.1. I have taken 4% germanium doped fused silica for the core of the fiber and 1% fluorine-doped fused silica in the cladding portion.

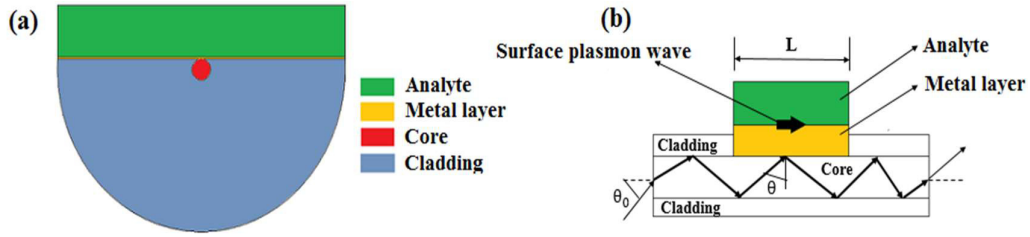

Fig. 2.1 Schematic of **(a)** the cross-section **(b)** the side views of the proposed single mode optical fiber sensor.

Refractive index of core and cladding depends on the wavelength which is determined by the Sellmeier's formula.

$$n^2(\lambda) = 1 + \frac{G_1\lambda^2}{\lambda^2 - H_1^2} + \frac{G_2\lambda^2}{\lambda^2 - H_2^2} + \frac{G_3\lambda^2}{\lambda^2 - H_3^2} \quad (2.1)$$

Where λ represents the light wavelength in μm and G_1, G_2, G_3, H_1, H_2 and H_3 are Sellmeier's coefficients. For Ge-doped silica, the values are $G_1 = 0.6867$, $G_2 = 0.4348$, $G_3 = 0.8966$, $H_1 = 0.07268$ μm, $H_2 = 0.1151$ μm, and $H_3 = 10.00$ μm, and for F-doped silica, the values are G_1=0.696166, $G_2 = 0.407942$, $G_3 = 0.897479$, $H_1 = 0.068404$ μm, $H_2 = 0.116241$ μm, and $H_3 = 9.89616$ μm[102 75].

The deposited metal Nano-layer on the un-cladded portion of the fiber is very useful for coupling between fiber core and analyte. I have used the Drude's model for dielectric constant of the metals as given;

$$\in_m(\lambda) = \in_{real\ part} + i \in_{imaginary\ part} = 1 + \frac{\lambda^2\lambda_c}{\lambda_p^2(\lambda_c + i\lambda)} \quad (2.2)$$

Where $\lambda_c$and λ_p represent the collision and plasma wavelengths of the metal. Collision wavelengths are $\lambda_c = 8.934\times10^{-6}$ m, 1.761×10^{-5} m, 4.085×10^{-5} m, and the plasma wavelengths are λ_p= 1.682×10^{-7} m, 1.454×10^{-7} m, 1.361×10^{-7} m for the metals Au, Ag, and Cu, respectively[103].

Analyte is taken in contact with the metal surface. RI and dielectric constant of the analyte are n_a and ϵ_a, respectively. The notation $n_1$is RI of fiber core and ϵ_m is metal dielectric constant. The surface plasmon resonance condition is given by the equation,

$$\frac{2\pi}{\lambda} n_1 \sin\theta = Re(K_{sp}) \quad (2.3)$$

Where the propagation constant $K_{sp} = \frac{\omega}{c}\sqrt{\frac{\epsilon_m\epsilon_a}{\epsilon_m+\epsilon_a}} = \frac{2\pi}{\lambda}\sqrt{\frac{\epsilon_m n_a^2}{\epsilon_m+n_a^2}}$ for the surface plasmon wave (SPW), and c is the velocity of light. The parameter θ is the angle of incident light, and $Re(K_{sp})$ represents the real value of propagation constant. The propagation constant can be modified by RI of the analyte, and hence the SPR condition is established at the different

wavelength. Shifting in resonance wavelength provides information about variation in the RI[77].

I have performed the simulation of mode analysis in optical fiber with the help of COMSOL Multiphysics modeling software. Propagation of electromagnetic field without any external electric charges and current in the optical fiber,

$$\Delta \times \boldsymbol{E}(r,\omega) = j\omega \boldsymbol{B}(r,\omega) \tag{2.4}$$

$$\Delta \times \boldsymbol{H}(r,\omega) = -j\omega \boldsymbol{D}(r,\omega) \tag{2.5}$$

Here, the notations ***E*, *B*, *H*** and ***D*** represent electric field, magnetic induction, magnetic field, dielectric field, respectively. The notations r and ω describe the position vector and angular frequency, respectively. It is also supposed the electromagnetic field justify the constitutive relations for a linear, isotropic and nonmagnetic media are following,

$$\boldsymbol{D}(r,\omega) = \tilde{\in}_r \in_0 \boldsymbol{E}(r,\omega) \tag{2.6}$$

$$\boldsymbol{B}(r,\omega) = \mu_0 \boldsymbol{H}(r,\omega) \tag{2.7}$$

Where $\in_0$ is permittivity and μ_0 is permeability in the free space and $\tilde{\in}_r$ represent the material-dependent relative permittivity. Using the above equations, I determine the Fourier component by the wave equation[104]

$$\nabla \times [\nabla \times \boldsymbol{E}(r,\omega) - k_0^2\, \tilde{\in}_r\,(r,\omega)]\boldsymbol{E}(r,\omega) = 0 \tag{2.8}$$

Where $k_0(\omega/c)$ is the propagation vector and c is represents the light velocity. $\tilde{\in}_r\,(r,\omega)$ denotes relative permittivity of the material.

This term is combination of the real value of permittivity ($\in_r$) and ohmic conductivity $\sigma(r,\omega)$ of the material.

$$\tilde{\in}_r\,(r,\omega) = \in_r - j\frac{\sigma(r,\omega)}{\omega \in_0} \tag{2.9}$$

The solution for Fourier component of electric field wave equation,

$$\boldsymbol{E}(r,\omega) = \boldsymbol{E}(r_\perp,\omega)e^{(jk_z \cdot z)} \tag{2.10}$$

Where $r_\perp$ and $E(r_\perp, \omega)$ are the position vector and electric field amplitude, respectively and both have direction perpendicular to the optical axis. $k_z(= k_0 n_{eff})$ is the relation between wavenumber of the mode in the optical axis (and total wavenumber (k_0). Where, n_{eff} $(= Re(n_{eff}) + iIm(n_{eff}))$ is the effective RI. Imaginary part $Im(n_{eff})$ characterizes the extinction coefficient. Optical power flow in the optical fiber is described by the real value of time-average pointing vector,

$$\boldsymbol{S} = \frac{1}{2} Re(\boldsymbol{E} \times \boldsymbol{H}) = \frac{1}{2} Re(e \times h) e^{-\alpha z} \tag{2.11}$$

Where α $(= 2Im(n_{eff})k_0)$ represents the power absorption coefficient. Confinement loss is the logarithm quantity which depends on the total wavenumber ($k_0 = 2\pi/\lambda$) and the imaginary part of the effective RI[76].

$$\alpha_{dB} = \frac{10}{ln10}\alpha L = \frac{40\pi}{(ln10).\lambda}.Im(n_{eff}).L$$

$$\alpha_{dB/cm} = 54.575 \times \frac{Im(n_{eff})}{\lambda} \times 10^4 \ (dB/cm) \tag{2.12}$$

Where λ denotes light wavelength in μm and $L = 1cm$ is the length of sensing part of the fiber.

2.3 Numerical results and discussion

In the proposed SPR based optical fiber sensor, the sensing part is consisted of a core-metallic Nano layer-analyte. The mechanism of sensing can be described as the analyte RI changes and their interaction with the metallic layer. I have calculated the SPR wavelengths for different refractive index. For the simulation study, I have considered the sensing length 1 cm and analyte RI from 1.33 to 1.42. The main mechanism of the SPR sensors is the distribution of the field of TM mode light in the core of the fiber. By the incoming wave evanescent fields, metal surface electrons are easily excited, and the surface plasmon wave is generated on the optical fiber surface. Distributions of the electric field in the guided core,

surface plasmon polaritons (SPP), and TM mode coupling in the fiber are shown in the insets of Fig. 2.2**.** The value of $Re(n_{eff})$ and confinement loss spectra for the Au layer of 40 nm with analyte RI 1.37. In the figure., the black line shows the real value of the coupling mode index, and the red line represents the confinement loss. The confinement loss is generated by the imaginary part of the coupling mode index using equation 2.12.

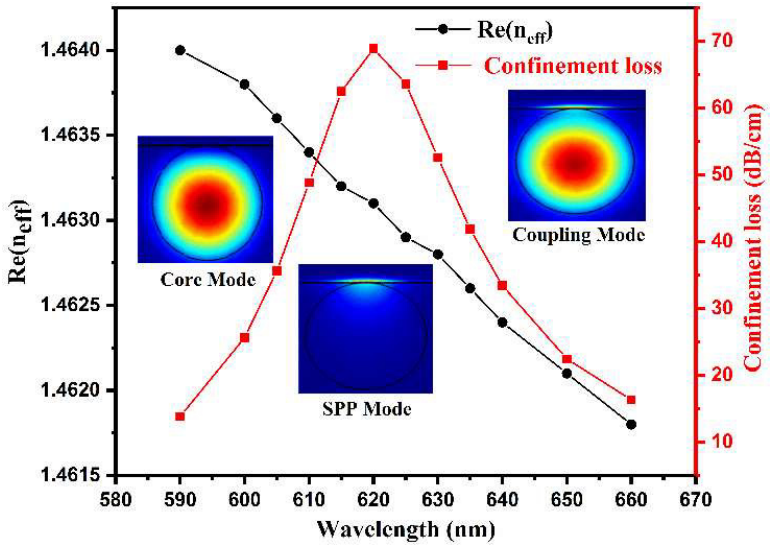

Fig. 2.2 Variations of real value of effective index $\boldsymbol{Re(n_{eff})}$ of coupling mode and confinement loss with wavelength for 40 nm Au layer with analyte RI 1.37.

I observe that the real value decreases with the wavelength, and the imaginary value of the coupling mode index initially increase with the wavelength and start continuously decreases after maximum resonance condition. The wavelength at which I have found maximum value of the imaginary effective index of coupling mode is called resonance wavelength. The real part of the effective refractive index $Re(n_{eff})$ represents the refractive index in the conventional form and the real value of time-average pointing vector, i.e., it is directly related to the wavelength and deceases linearly with wavelength, because most of the energy of incident light guided in the core which linearly decreases with the wavelength. The imaginary part of the effective refractive $Im(n_{eff})$ is closely related to the losses in the fiber and it is represented as the confinement loss. In step index optical fiber, the numerical aperture (NA)

is also an important characteristic, which is determined by the relative magnitudes of the refractive indices in the core and in the cladding. It exhibits the light-collecting properties of the fiber. NA can be calculated from the expression as[75]

$$NA = \sqrt{(n_{core}^2 - n_{cladding}^2)} \tag{2.13}$$

The variations of the NA different cladding conditions are shown in the Fig. 2.3. In the inset of Fig. 2.3, I have depicted the variation of numerical aperture with wavelength for without removed cladding of normal fiber. The variation of NA exponentially decreases with increasing the wavelength. For the different metal-coated fibers, the NAs also decreases with increasing the wavelength, but the variations are not in similar way as the normal fiber.

The NA values for all the considered metal-coated fiber are higher than the normal fiber. For the different coated metals, NA values are maximum for the Cu metal and minimum for the Au metals as seen in the figure. At the lower wavelength, the NA values have approximately the same values for all the cases.

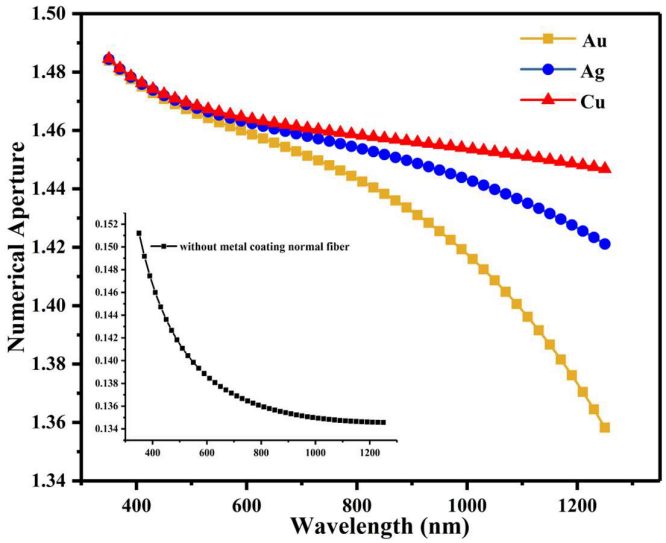

Fig. 2.3 Variations of numerical aperture (NA) with wavelength for different metal (Cu, Ag, and Au)-coated fibers and normal fiber.

Moreover, another parameter coupling efficiency of the fiber is defined as a result of the amount of power emitted from an optical source that can be coupled into a fiber. Because the

optical power-carrying capacity of the fiber is linearly proportional to the square of its numerical aperture, it is desirable to have a fiber with a large numerical aperture for the potential applications. Thus, I observe the linear variations in the coupling efficiency with respect to the change of NA of the proposed fiber design. According to the coupling efficiency condition, if the NA values of the coated fibers are more than one, then the coupling efficiency is one. Therefore, the coupling efficiencies are considered equal to one for all the cases of considered plasmonic metals.

Resonance wavelength and confinement loss spectra with the variations of analyte refractive indices are shown in Fig. 2.4 for the different metals Au, Ag, and Cu. Figure reveals the variations of the confinement loss and resonance wavelength with the different refractive indices of the analytes for 50 nm of Au, Ag, and Cu as plasmonic layers. The confinement loss and resonance wavelength both continuously increase with the analyte refractive index for all three plasmonic metals. The loss values for the plasmonic layer of Cu metal are greater than Au and Ag metals. The resonance wavelength values for Au metal have more shifting in longer wavelength region compared to Ag and Cu metals, and it has higher values for the Au layer. For the small value of the analyte RI, resonance condition contented at a smaller wavelength because of the small value of the real part of the SPW propagation constant[105]. Similar resonance conditions satisfied for larger refractive indices of the analyte.

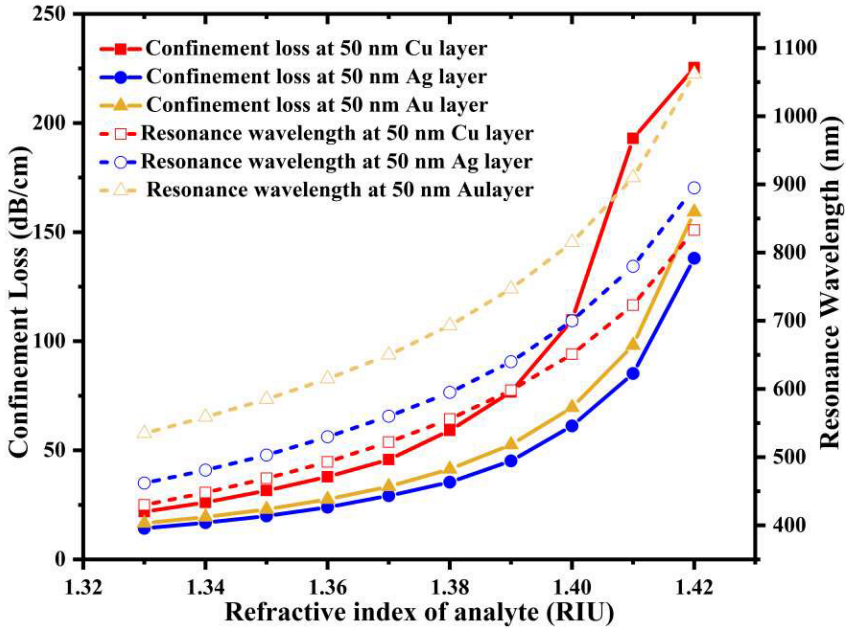

Fig. 2.4 Confinement loss spectra and resonance wavelengths variation with the RIs of analytes for 50 nm thick Au, Ag, and Cu metals layer.

Resonance wavelengths magnify with the analyte refractive indices for all cases of the layer thicknesses. The peak values of confinement loss increase with analyte refractive indices from 1.33 to 1.42. Thus, the coupling condition increases with an increase of the analyte RI. This condition can be manipulated for different types of considered metallic layers. Resonance wavelength and confinement loss can be tuned by considering the different analytes and different plasmonic metals.

Confinement loss does not only depend on wavelength but also depends on the imaginary part of effective refractive index $Im(n_{eff})$ which depends on many parameters like plasmonic material, metal thickness, analyte refractive index, and fiber design. Fig. 2.4 shows that the confinement losses for the considered plasmonic metals increase with the analyte RI ranging from 1.33 to 1.42 due to the coupling between SPP mode and core mode wavelength. For Cu metal, the confinement loss rapidly increases with analyte RI ranging from 1.39 to 1.42 due to strong coupling. I observe that the confinement loss value increases with the analyte RI if all other parameters are constant. The mathematical Eq. 2.3 explains the

resonance wavelength shifting in the longer wavelength region with increase of the analyte refractive index. The real value of propagation constant $Re(K_{sp})$ of surface plasmon wave will be smaller for the small value of analyte refractive indices, and hence, its resonance condition is satisfied at a smaller wavelength. Similarly, for the higher value of the analyte refractive index, the resonance condition is satisfied at a longer wavelength due to the higher real value of $Re(K_{sp})$ [77].

The performances of the optical sensor are generally characterized by the parameters such as sensitivity, figure of merit (FOM), and resolution. The sensitivity of the optical fiber sensor obtained according to[76]

$$S_\lambda = \frac{\Delta\lambda_{peak}}{\Delta n_{analyte}} \quad (nm/RIU) \tag{2.13}$$

Where $\Delta\lambda_{peak}$ and $\Delta n_{analyte}$ are the difference of resonance peak wavelength and refractive indices for any two analytes, respectively.

Maximum sensitivities of the proposed sensor with various layer thicknesses of metals Au, Ag, and Cu for analyte RI from 1.41 to 1.42 are shown in Fig. 2.5(a). Fig. 2.5(b) depicts the average sensitivity for the analyte RI from 1.33 to 1.42 for the same parameter of the metallic layer. Sensitivity magnifies with layer thicknesses of metals, and sensitivity for the Au layer is found higher than Ag and Cu layers because of the real part of the dielectric constant of Au has the higher value for all wavelengths[105]. These conditions occur due to the real value of propagation constant, and it is responsible for changing of the resonance wavelength. Shifting of resonance wavelengths increases with analyte refractive indices, so the sensitivity increases. Numerical value of maximum sensitivity and average sensitivity for Au, Ag, and Cu at different thick layers are listed in table 2.1.

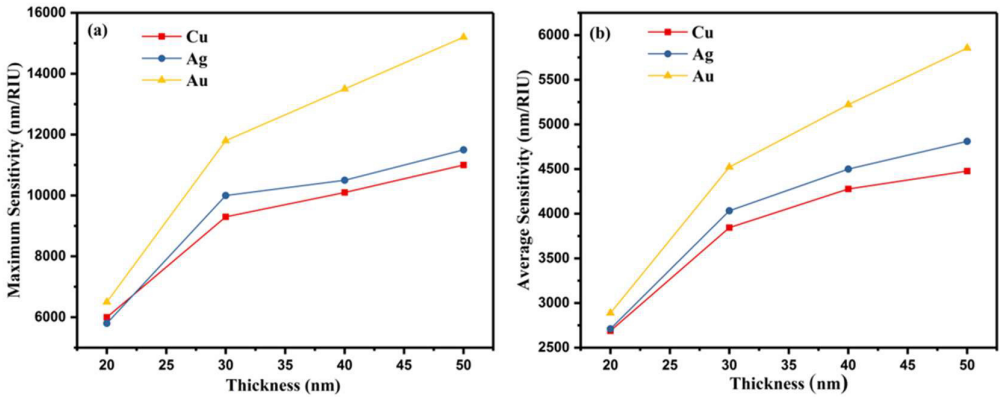

Fig. 2.5 Variations of **(a)** maximum sensitivity for n_a= 1.41 - 1.42, **(b)** average sensitivity for n_a = 1.33 - 1.42, with various layer thicknesses of metals Au, Ag and Cu.

Table 2.1. Sensitivity of the proposed optical fibre sensor with metals Au, Ag and Cu for various layer thicknesses.

Metal	**Au**				**Ag**				**Cu**			
Thickness(nm)	20	30	40	50	20	30	40	50	20	30	40	50
Maximum sensitivity(nm/RIU) for RI = 1.41-1.42	6500	11800	13500	15200	5800	10000	10500	11500	6000	9300	10100	11000
Average sensitivity (nm/RIU) for RI = 1.33-1.42	2888	4522	5222	5855	2711	4033	4500	4811	2628	3844	4277	4477

For better understanding the effect of different metals on the sensitivity of the different analytes, I have revealed the variations of the sensitivity for various analytes with different metals of layer thickness 50 nm in Fig. 2.6. I observe that the sensitivity exponentially increases with increase of the analyte refractive indices for all cases. The maximum sensitivity form the proposed optical fiber sensor is obtained for Au layer composed fiber and then Ag and Cu, respectively. To obtained the maximum sensitivity for the considered deign of optical fiber sensor, the optimize metals thickness and analyte refractive index should be identified for higher values, but it should not be cost effective and sensing utility.

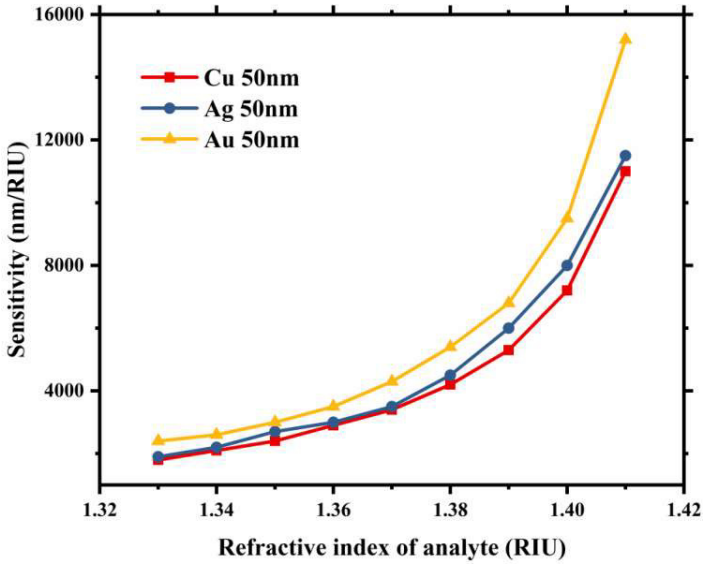

Fig. 2.6 Sensitivity variations with the analyte refractive indices for 50 nm thick Au, Ag and Cu layers.

Figure of merit (FOM) is also an interesting performance parameter of the optical fiber sensor. The FWHM (full width at half maxima) represents the width of the curve at half of its maximum height. It's a crucial parameter in physics, as it indicates the resolution or precision of a measurement system. The smaller the FWHM, the sharper or more precise the peak or distribution. The FOM is represented by the ratio of the sensitivity and FWHM which can be calculated by using equation[106]

$$FOM = \frac{S(\lambda)}{FWHM} \quad (RIU^{-1}) \tag{2.14}$$

Another interesting parameter of the fiber sensor is resolution which determines the variation of wavelength shifting with very small change of refractive index of analytes. Resolution of the sensor can be calculated by the equation[76]

$$R = \frac{\Delta\lambda_{min}}{S(\lambda)} \ (RIU) \tag{2.15}$$

Where $\Delta\lambda_{min}$ and $S(\lambda)$ are minimum spectral resolution and sensitivity of the fiber sensor, respectively[76].

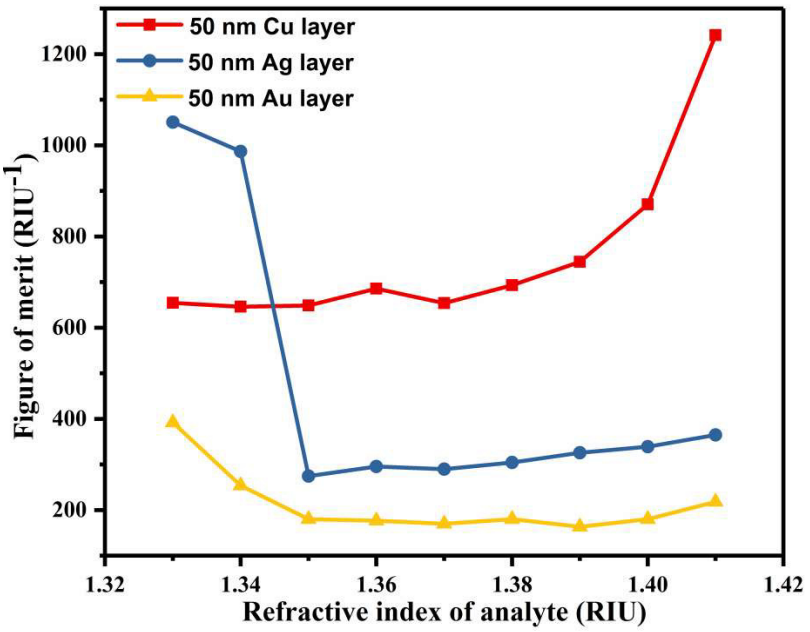

Fig. 2.7 Variations of FOM with the RIs of analyte for Au, Ag, and Cu layers of 50 nm.

Fig. 2.7 reveals the variation of the figure of merit (FOM) with various analyte refractive indices for the plasmonic metals Au, Ag, and Cu of layer thickness 50 nm. I observe that the FOM for Ag rapidly decreases for analyte RI from 1.33 to 1.35, and then, it slowly changes with the variation of analyte RI from 1.35 to 1.41. Thus, the FOM enhancement can be realized when the refractive index of analyte is low. In the case of Au, the FOM slowly decreases with analyte refractive index from 1.33 to 1.35, and after that, it has changed with very minimal values with analyte refractive indices. The variations of the FOM for Cu show the contravariant result. It increases with increasing the values of analyte refractive index. The FOM values for the plasmonic Cu layer are higher compared to Ag and Au metal layers, because the full width half maxima (FWHM) values for Cu layer are smaller than Ag and Au metal layers. The numerical values of resonance wavelength, sensitivity, FWHM, and FOM of the proposed sensor with 50 nm of Au layer for different RIs of analyte are listed in Table 2.2.

Table 2.2 Figure of merit of the introduced sensor for various analytes with 50 nm of Au layer.

Analyte RI	Resonance Wavelength (nm)	Sensitivity (nm/RIU)	FWHM (nm)	FOM (RIU^{-1})
1.33	535	2400	6.12	392.15
1.34	559	2600	10.25	253.66
1.35	585	3000	16.66	180.07
1.36	615	3500	19.80	176.77
1.37	650	4300	25.29	170.02
1.38	693	5400	29.95	180.30
1.39	747	6800	41.56	163.61
1.40	815	9500	52.75	180.09
1.41	910	15200	69.72	218.01
1.42	1062	----	85.57	----

The comparisons of my proposed SPR-based D-shaped single-mode optical fiber sensor with some previously reported SPR, LSPR (localized surface plasmon resonance) and LMR (lossy mode resonance) based works are shown in Table 2.3. I observe that the proposed optical fiber sensor has better sensitivity and resolution for effectively sensing performance of analyte of RI ranging 1.33 to 1.42.

Table 2.3 Comparison of the proposed SPR based optical fiber sensor.

Reference	Numerical method	Sensitivity (nm/RIU)	Resolution (RIU)	RI Range
77	Theoretical FEM SPR	3161	---	1.30-1.37
107	Experimental LMR	2280	---	1.3334-1.4471
108	Experimental SPR	1650	---	1.33-1.37
109	Experimental SPR	4583.4	---	1.36-1.41
110	Experimental LSPR	3389	---	1.34-38
111	Simulation FEM SPR	2765	---	1.332-1422
This study	Simulation FEM SPR	5855	1.708×10^{-5}	1.33-1.42

In the literature, most of the articles have been reported on the photonic crystal fiber (PCF) and multi-mode optical fiber. The analysis and design of the PCF and multimode optical fiber-based sensors are complicated for both the theoretically and experimentally cases. The single mode fiber is more flexible and efficient compared to the PCF and multi-mode fiber, and it has been utilized for different potential applications such as gas sensor[112] long period fiber grating gas sensor[113] strain and temperature sensor[114 115] and organic chemical and bio-chemical[116 117 118]. In my proposed work, I have analyzed the single mode SPR based highly sensitive D-shaped optical fiber RI sensor and compared their results for three different plasmonic metals and structural parameters. I have achieved longer resonance wavelength, higher sensitivity, and maximum resolution with low loss for longer analyte refractive index range. Therefore, the proposed fiber sensor may be very useful and efficient in the chemical and biological field for sensing based on the RI.

2.4 Conclusion

In this work, SPR-based highly sensitive D-shaped optical fiber RI sensor with a single layer of metal has been numerically investigated. I have considered the metals Au, Ag, and Cu, for the excitation of plasmon surface wave. O observed that the sensitivity increases with increasing the analyte RI from 1.33 to 1.42. Sensitivity increases with an increment of the layer thickness of metals. The proposed sensor with an Au layer of 50 nm illustrates the average sensitivity 5855 nm/RIU, maximum sensitivity 15,200 nm/ RIU, and resolution 1.780×10^{-5} RIU. The introduced sensor with separate Ag and Cu layers of 50 nm shows the average sensitivities 4811 nm/RIU and 4477 nm/RIU, maximum sensitivities 11,500 nm/RIU and 11,000 nm/RIU, and resolutions 2.078×10^{-5} RIU and 2.233×10^{-5} RIU, respectively. I observe that the overall performance of the introduced sensor with an Au layer is higher than that consisted of Ag and Cu layers. FOM of the proposed sensor is obtained in the range from 392.15 to 218.01 RIU^{-1} with various RI of analyte for 50 nm Au layer. This fiber sensor is very useful in the chemical and biological field for sensing based on the RI of the sample.